NATIONAL RADIO ASTRONOMY OBSERVATORY
Green Bank, West Virginia

Electronics Division Internal Report No. 17

APPLICATION OF THE ANTENNA TOLERANCE
THEORY TO THE NRAO 85-FOOT AND 300-FOOT
TELESCOPES

P. G. Mezger

AUGUST 1963

APPLICATION OF THE ANTENNA TOLERANCE THEORY TO THE NRAO 85-FOOT AND 300-FOOT TELESCOPES

P. G. Mezger

1. Introduction

The term "Antenna Tolerance Theory" was first introduced by Bracewell [1]. The importance of antenna tolerance theory for the construction of very large antennas is obvious.

In this report we are only concerned with two kinds of errors in parabolic antennas:

    1. Defocusing of the primary feed.

    2. Random deviations of the parabolic reflector from an ideal paraboloid.

In section 2 we will give a short review of the theoretical results obtained by various authors for these two cases. As far as we know, only two attempts have so far been made to check these results experimentally with very large antennas [10] [11]. Since the NRAO operates a 85-foot and a 300-foot antenna, whose reflectors have been measured mechanically with very high accuracy, and since on the other hand feeds and receivers for various frequencies are available, we think it was a good opportunity to compare the performance of the antennas with the theoretically predicted behavior.

The experimental results communicated in this report are neither complete nor are they obtained with the highest possible accuracy. The reason is that this report is not considered to be a final report, but rather a working report to show what we planned to do and to stimulate, if possible, a helpful discussion of our future work in this field.

Some important measurements, especially concerning the 300-foot telescope, have been obtained by our colleagues, who will be mentioned in connection with the corresponding results.

2. Short Review and Some Results of the Tolerance Theory of Paraboloid Antennas

Let us start considering an ideal parabolic reflector and a primary feed with a well defined phase center. When the phase center of the feed coincides with the focal point of the reflector we have the maximum gain G_o, the half power beamwidth (HPBW) Θ_A, and the squint angle between electrical and mechanical axes $\Theta = 0$. A displacement

of the phase center may be decomposed in a displacement Δf_{rad} in radial direction (or in the focal plane) and in a displacement Δf_{ax} along the focal axis of the paraboloid. The axial defocusing causes a divergent beam, if the phase center is moved towards the reflector and a convergent beam if the phase center is moved in the opposite direction. Yang [2] calculated the following expression for the gain variation for a constant reflector illumination

$$(1a) \qquad G/G_o = \left[\frac{\sin u/2}{u/2} \right]^2$$

with $u/2 = \pi (1 - \cos \psi) \Delta f_{ax}/\lambda$ and ψ = aperture angle of the antenna. This result means that the gain variation only depends on the amount but not on the direction of the axial defocusing. This is of some importance for the focusing of the feed, as will be shown in section IV. The gain variation will increase for a given ration $\Delta f_{ax}/\lambda$ with increasing aperture angle ψ. Bracewell [1], who treats the problems in his paper from a more physical and qualitative point of view gives for the gain variation due to an axial defocusing the expression

$$(1b) \qquad G/G_o = 1 - \Delta^2/12$$

where Δ means the maximal phase error between center and edge of the aperture. With $\Delta = 2\pi (1 - \cos \psi) \Delta f_{ax}/\lambda$ it may easily be shown that equation (1b) is the quadratic approximation of equation (1a).

For comparatively small radial defocusing the gain of the antenna is not changed but a "squint" is produced, which means that the electrical axis of the antenna deviates from the mechanical axis by an angle Θ, measured in the same plane but in the opposite direction of the radial defocusing. In the case of a flat reflector the squint angle would be related to the radial defocusing by $\Theta' = \arctan (\Delta f_{ax}/f)$ where f is the focal length of the antenna. For a paraboloidal reflector the true squint angle Θ is smaller than Θ' by a factor of $B \leq 1$

$$(2) \qquad \Theta = B(f/D) \, \Theta' = B(f/D) \, \arctan (\Delta f_{ax}/f)$$

The beam deviation factor B is a function of the f/D (D   diameter of the aperture) value (or the aperture angle) of the antenna.   The beam deviation factor B is given by Silver ([3] p. 488) for the case that the feed is moved on a circle around the vertex of the paraboloid. It is not mentioned for which illumination the curve has been calculated.

Kelleher, et al [4] give an equation for the calculation of the beam factor with a given f/D

$$(3) \qquad B = 1 - \frac{\int_0^{x_0} g(x) \frac{x^4}{4 + x^2} dx}{\int_0^{x_0} g(x) x^2 dx}$$

In this equation x_0 = D/2f and g(x) is the amplitude illumination along the x-plane (z = 0). It may be seen from equation (3) that for a given antenna, the beam factor B approaches 1 with increasing tapering of the feed pattern.   This result is interesting for those applications in radio astronomy where the beam of an antenna is moved by displacing of the feed radially.

For a main beam squint more than the HPBW of the antenna, the decrease in gain may become noticeable, depending on f/D (Silver [3], p. 88); also, the HPBW will increase correspondingly.

The deviations of the points from the best fitting paraboloid measured in a direction perpendicular to the paraboloid will be called the deviation D_i of the point i.   The definition of the best fitting paraboloid does not necessarily imply that the mean value $m = \sum_{i=1}^{N} D_i$ vanishes, but m = 0 may be assumed in the interesting cases as will be shown in section III.

The basic work in the theoretical treatment of random deviations of a parabolic reflector from an ideal paraboloid has been done by Ruze [5].   He inserts a position dependent phase error $\delta(\vec{r})$ in the integral representation of the far field pattern.   For the phase error itself, he assumes a gaussian distribution.   Since for relatively flat reflectors the relation

$$(5) \qquad \delta = 2D \frac{2\pi}{\lambda}$$

between the deviation D and the corresponding phase error δ holds, Ruze's assumption means that the deviations D of the reflector may be represented by the function

$$(6) \qquad W(D) = \frac{1}{(2\pi\overline{D^2})^{1/2}} \exp\left\{ - D^2/2\overline{D^2} \right\}$$

Let τ be the distance between two points on the parabolic reflector. For large values of τ the deviations of the reflector, and hence the phase errors are then uncorrelated, whereas for $\tau \approx 0$ the mean square value of the phase error is obviously zero. To account for this fact, Ruze introduces the following relation for the mean square value of the phase errors between points located at a distance τ on the paraboloid

$$(7) \qquad \delta(\tau)^2 = \delta^2 [1 - \exp(-\tau^2/C^2)]$$

C is defined as a correlation interval that is the average distance where the phase errors and the deviations become independent. Ruze gives the rigorous solution of the problem and the following important approximations:

   a. For a correlation interval small compared to the wavelength, and for small reflector errors the reduction in gain is

$$(8a) \qquad G/G_o = 1 - \frac{3}{4} \overline{\delta^2} \frac{c^2\pi^2}{\lambda^2} = 1 - 12\pi^4 \frac{\overline{D^2} c^2}{\lambda^2} \qquad \frac{c}{\lambda} \ll 1$$

   b. For a large correlation interval the gain reduction is given by

$$(8b) \qquad G/G_o = \exp(-\overline{\delta^2}) = \exp[-16\pi^2 \frac{\overline{D^2}}{\lambda^2}] \qquad \frac{c}{\lambda} \gg 1$$

where the relation (5) has been used to replace the mean square value of the phase error $\overline{\delta^2}$ by the mean square value of the surface deviation $\overline{D^2}$. It should be remembered that Ruze obtained these results by averaging over an ensemble of similar paraboloid antennas. Correspondingly, the results of equations (8a) and (8b) do not relate a mean square deviation $\overline{D^2}$ of the paraboloid with a well defined gain reduction, but rather predict the average gain reduction of an ensemble of similar antennas, whose reflectors have the same mean square deviations $\overline{D^2}$.

Of great importance for all practical applications is the dependence of the gain reduction not only on the wavelength but also on the ratio between the correlation interval c and the wavelength. It can be shown that "rough" reflector surfaces do hardly affect the performance of the antenna. Bracewell [1] shows qualitatively in his paper the effect of the variation (= correlation) of the errors over the aperture. Whereas rapidly varying errors reduce the gain, as well as the directivity D, of the antenna and hence the antenna beam solid angle $\Omega = 4\pi/D$, the HPBW is not affected. With increasing correlation interval (slowly varying errors) the scattered radiation becomes more directive and first the attenuation of the near sidelobes and eventually the main beam itself will be affected by the surface deviations. This is in good agreement with the practical experience that with decreasing wavelength both the antenna efficiency and the attenuation of the first sidelobes decrease, and consequently the stray factor of the antenna increases.

3. Results of a Photogrammetric Calibration of the 85-Foot and the 300-Foot Telescopes*

The paraboloid reflectors of the two telescopes have been measured just in the same way as defined in section 2. Figure 1 shows the distribution of the target points on a plane projection of the parabolic reflector in the case of the 85-foot telescope. The positions of these target points in a x, y, z-coordinate system have been obtained by a photogrammetric method, and the best fitting paraboloid through these points has been determined by the method of least squares. These photogrammetric measurements have been made for the 85-foot telescope at the zenith angles z = 0° and z = 90°, respectively, and for the 300-foot telescope at the zenith angles z = 0°, 30° and 51° 23' 40", respectively. We start our computations from the listed deviations D_i of the target points i from the best fitting paraboloid. Let N be the total number of all target points used for an individual surface calibration. Then we calculate the mean value

$$(9) \qquad m = \overline{D} = \frac{1}{N} \sum_{i=1}^{N} D_i$$

and the RMS deviation

$$(10) \qquad s = \sqrt{\overline{D^2}} = \frac{1}{\sqrt{N}} \left[\sum_{i=1}^{N} D_i^2 \right]^{1/2}$$

---

* The photogrammetric calibration of the two telescopes has been done by D. Brown Associates, Inc., Eau Gallie, Florida.

The results of these calculations are listed in Table 1.

Then the numbers N_i of deviations, lying in a range between D_i and $D_i + \Delta D$ have been counted. The normalized values N_i/N are plotted in Figures 2a - 6a. With the values m, s, and N of Table 1 the corresponding gauss distributions

$$(11) \qquad G(D;h) = \frac{h}{\sqrt{\pi}} \left\{ \exp -h^2 (D-m)^2 \right\}$$

with

$$h = \frac{1}{s\sqrt{2}} \left(\frac{N-1}{N} \right)^{1/2}$$

have been calculated and plotted in the corresponding diagrams. (For the statistical definitions used here, see for example [6]).

As may be seen in Figure 1, the target points are not equally spaced on the paraboloid but the surface elements represented by an individual target point attain a smallest value at a distance of about $2R_o/3$ of the vertex (measured in the aperture plane with R_o the radius of the aperture). To account for this fact we have calculated the mean square deviations according to equation (10) of all target points lying in a ring-shaped zone on the paraboloid defined by $R_i \leq R \leq R_{i+1}$ in the aperture plane.

The results of these calculations are represented in Figures 2b - 6b. As may be seen, the mean square deviations of the individual ring-shaped zones vary considerably. In the case of the 85-foot telescope, the mean square deviations increase with increasing distance of the vertex. In the case of the 300-foot telescope, however, the biggest deviations are generally found in the neighborhood of the vertex.

The measured target points within one ring-shaped zone represent approximately the same surface element. If $\overline{D_k^2}$ is the mean square deviation of the kth zone, F_k the corresponding surface of this zone on the paraboloid, then the weighted mean square deviation is

$$(12) \qquad \overline{D^2} = \frac{1}{F} \sum_k \overline{D_k^2} \, F_k$$

- 7 -

TABLE 1

	TELESCOPE	85-FOOT		300-FOOT		
Zenith angle z =		0°	90°	0°	30°	51° 23' 40"
N = number of independent measurements		243	244	293	291	293
Mean value $m = \bar{D}$		-0.009 mm	0.091 mm	0.546 mm	-0.041 mm	-0.229 mm
RMS deviation $s = \sqrt{\bar{D^2}}$		3.164 mm	5.709 mm	10.717 mm	12.701 mm	9.466 mm
Weighted RMS deviation according to eq. (13)		2.751 mm	4.173 mm	12.437 mm	12.627 mm	10.866 mm
Focal length of best fitting paraboloid		10.937 ± 0.0018 m	10.896 ± 0.00046 m	38.948 ± 0.0027 m	39.008 ± 0.0034 m	39.059 ± 0.0036 m

Ruze has obtained equations (8a) and (8b) with the assumption of a constant illumination of the reflector. In practice, however, the primary feed pattern is tapered in order to reduce spillover, and to improve the sidelobe attenuation. This means that a deviation at the edge of the reflector contributes much less to the gain reduction than does the same deviation in the vicinity of the vertex. Figure 7 shows the normalized primary pattern of two horn feeds used with the 85-foot telescope at 1.4 and 7.4 GHz. The primary pattern of the two feeds used with the 300-foot telescope at 0.75 and 1.4 GHz, respectively, do not deviate much from this curve. With the aid of these normalized patterns we may define the weight p_k for the kth zone. Consequently, the weighted mean square deviation, considering the taper, becomes

$$(13) \qquad \overline{D^2} = \frac{\sum\limits_k \overline{D_k^2}\, F_k\, p_k}{\sum\limits_k F_k\, p_k}$$

The square root of this value is listed in Table 1. The numerical results are interesting because the RMS deviation is reduced by the weighting process in the case of the 85-foot telescope, whereas the RMS deviation of the 300-foot telescope is amplified by the weighting process.

4. Comparison Between Theory and Experimental Results

a. Defocusing

The variation of the gain as a function of the axial position of the feed's phase center has been measured with the 85-foot antenna at various frequencies. Figures 8a and b show some results obtained at 4 and 6 cm wavelength, respectively. The curves have been calculated from equation (1a) for an aperture angle $\psi = 120°$ of the 85-foot paraboloid. First the feed was adjusted for optimum gain (= maximum antenna temperature of a radio source). Then the position of the feed was changed by known amounts Δf_{ax} and the corresponding antenna temperature of the radio source was measured. In Figures 8a and b the defocusing distance Δf_{ax} has been normalized to the wavelength λ, and the measured antenna temperatures have been normalized to the optimum antenna temperature of the source $\Delta f_{ax} = 0$. These results confirm the validity of equation (1a),

at least for a defocusing range of $\pm \lambda$, and show that for a small axial defocusing the gain depends only on the amount but not on the direction of defocusing. Therefore, the focusing of the feed can be done very easily by measuring the gain variation curve and determining its symmetry axis.

The effect of radial defocusing has been studied with the 300-foot telescope. Theoretical values for the beam factor have been obtained from Silver's curve [3] and from equation (3), respectively. Equation (3) has been evaluated for a constant amplitude illumination (g (x) $\equiv$ 1] and for a normally tapered primary pattern ($g(0)/g(x_o) \triangleq 14.5$ db). The results are compiled in Table 2.

TABLE 2

		Beam factor B
Silver	[3]	0.885
Kelleher, et al [4] constant illunination		0.826
Tapered 14.5 db down at the edge		0.857
Burke [7] experimental value		0.873

Burke's value has been obtained by displacing
the feed at a certain well defined amount
($\approx \pm$ 2^{m}20^s in RA) and determining the passage
time of Cas A.

Considering the fact that the tapering of the feed used in Burke's measurement is not known, the agreement between theory and experiment seems to be satisfactory. The dependence of the gain on the radial defocusing of the feed has also been investigated with the 300-foot telescope. To be independent of possible declination errors, the 300-foot antenna scanned the radio source in declination while tracking it continuously in RA. Figure 9 shows the results obtained for various radio sources. Again the antenna temperatures of the sources, measured as a function of the beam angle Θ (which has been normalized to the antenna HPBW Θ_A), have been normalized to the values measured at zero deflection ($\Theta = 0$). The theoretical curve has been obtained by extrapolating Silver's

curve [3] for a ratio $f/D = 0.42$ of the 85-foot antenna. For the beam tilted towards the west, the measured points follow approximately the theoretical values, whereas in the east the gain decreases more rapidly as predicted by theory. The obvious symmetry in the gain curve may possibly be a result of an inclination of the feed axis with respect to the reflector axis.

b. Random deviations of the parabolic reflector

The gain of the 85-foot antenna has been measured at four wavelengths between 21 cm and 4 cm, by measuring the antenna temperature of the radio source Cas A. To calculate the effective antenna area the relation has been used

$$(14) \qquad A = 2k \frac{T_A}{S_\nu} \left(1 + \frac{\Theta_S}{\Theta_E}\right)^{1/2} \left(1 + \frac{\Theta_S}{\Theta_H}\right)^{1/2}$$

Here
$\qquad k = 1.38 \cdot 10^{-23}$ Ws/°K - the Boltzmann's constant

$\qquad T_A$ = the maximum antenna temperature of the radio source

$\qquad \Theta_S = 3.7'$ - the HPBW of Cas A

$\qquad S_\nu$ = the flux density of Cas A at the frequency ν

S_ν may be determined from the value $S_{1.44 \text{ GHz}} = 247 \cdot 10^{-25}$ W/m²Hz and the spectral law $S \sim \nu^{-0.78}$, and Θ_E, Θ_H are the HPBW's in the main planes of the antenna.

The HPBW's of the antenna have been obtained from drift curves by applying a correction for the size of the radio sources used for these measurements. By assuming a gaussian shape of the main beam of the antenna $f_m = \exp\{-\xi^2/(0.6 \Theta_E)^2 - \eta^2/(0.6 \Theta_H)^2\}$, the main beam solid angle can be calculated from the relation $\Omega_m = 1.133 \Theta_E \Theta_H$. The antenna solid angle can be obtained from $\Omega = 41253 \cdot \lambda^2/(4\pi \cdot A)$. The main beam stray factor of the antenna is defined as

$$(15) \qquad \beta_m = \int_{4\pi} (f - f_m) \, d\Omega/\Omega = 1 - \Omega_m/\Omega$$

where f means the true antenna pattern f_m the gaussian main beam pattern and $\Omega = \int_{4\pi} f \cdot d\Omega$ the antenna solid angle. It may be shown that the relation

$$(16) \qquad G = \eta_R (1 - \beta_m) \frac{4\pi}{\Omega_m}$$

between the antenna gain G, main beam stray factor β_m, and main beam solid angle Ω_m holds. η_R means the radiation efficiency which accounts for losses in the feed and reflector.

The measured values for the 85-foot antenna and for the 300-foot antenna, respectively, have been compiled in Table 3. We have added in this list the efficiency at 1.8 cm wavelength, which has been measured by Barrett [9] with a similar antenna.

To compare these measurements with Ruze's theory we first have to decide the correlation interval C (eq. 7), at which the deviations of the paraboloid become independent. The contour map representation of the 85-foot reflector (Fig. 10) clearly shows that this correlation interval is large compared to all wavelengths λ at which measurements have been made. Therefore, the assumption $C/\lambda >> 1$ seems to be justified, and we may calculate the gain reduction as a function of wavelength from equation (8b).

For our purposes it is more convenient to rewrite equation (8a) in the form $\eta_A(\lambda) = \eta_{A_0} \exp(-\delta^2)$, where $\eta_A(\lambda)$ means the antenna efficiency as a function of wavelength and η_{A_0} is the antenna efficiency of the ideal parabolic reflector. To obtain this value η_{A_0} the logarithm of the measured values $\eta_A(\lambda)$ have been plotted against $1/\lambda^2$. The extrapolation of the curves give the following values:

TABLE 4

	85-foot antenna	300-foot antenna
$\eta_{A_0} = \eta_A(\lambda = \infty)$	59%	67%

Using these values and the weighted RMS deviations of the antenna reflectors from Table 1, we have calculated the antenna efficiency as a function of wavelength and plotted the resulting curves in Figures 11a and b. The measured values of the antenna efficiency from Table 3 have been inserted in the diagrams. The accuracy of the antenna efficiency measurements have been estimated to be $\pm$ 15%. The calculated and measured values of the antenna efficiency agree very well in the case of the 300-foot telescope; for the 85-foot telescope, however, the antenna efficiencies measured are higher than would be expected from the RMS deviations of the parabolic reflector.

TABLE 3

85-FOOT ANTENNA

Measurements made by	Wavelength λ/cm	Antenna efficiency η_A	HPBW/min arc min.	HPBW/min arc max.	Solid angle Antenna $\Omega/\square$	Solid angle Main beam $\Omega_m/\square$	Stray factor Main beam β_m
Wade [8] Mezger	21.1	0.58 0.54	35 36	35.8 36.7	$4.8 \cdot 10^{-1}$ $5.1 \cdot 10^{-1}$	$3.9 \cdot 10^{-1}$ $4.2 \cdot 10^{-1}$	0.19 0.18
Wade [8]	10	0.52	15.7	15.9	$1.2 \cdot 10^{-1}$	$7.9 \cdot 10^{-2}$	0.34
Mezger	6	0.45	10.8	10.8	$5.9 \cdot 10^{-2}$	$4.0 \cdot 10^{-2}$	0.32
Mezger	3.95	0.32	6.3	6.3	$3.1 \cdot 10^{-2}$	$1.2 \cdot 10^{-2}$	0.61
Barret [9]	1.8	0.25 *					

300-FOOT ANTENNA

Measurements made by	Wavelength λ/cm	Antenna efficiency η_A	HPBW/min arc min.	HPBW/min arc max.	Solid angle Antenna $\Omega/\square$	Solid angle Main beam $\Omega_m/\square$	Stray factor Main beam β_m
Wade [8]	40	0.59	18.5	18.5	$1.4 \cdot 10^{-1}$	$1.1 \cdot 10^{-1}$	0.22
Wade [8]	21.4	0.40	10.0	10.0	$5.7 \cdot 10^{-2}$	$3.1 \cdot 10^{-2}$	0.46

* In Figure 11a an earlier incorrect value of 10 percent has been used.

5. Discussion of the Results

As we have pointed out in the preceding section, experiment and theory agree very well, if the fact is considered that equation (8b) gives the average gain reduction for a large number of antennas with the same RMS deviation of its reflectors. To be able to compare the antenna efficiency measured at different wavelengths, the primary pattern of the feeds should be identical in all cases. This assumption is approximately correct in our case with the exception of the measurement at 6 cm wavelength, where a feed with a special design for high gain and low spillover has been used.

It is a striking feature in the case of the 85-foot antenna that the RMS deviation of the reflector increases more than 50% when the antenna is tilted from zenith to horizontal position, which leads to a large difference between the calculated antenna efficiency curves in Figure 11a.

Since all efficiency measurements with radio sources have been done at relatively high elevation angles, it is comprehensible that the measured values are closer to the curve calculated for zenith position. Not only the RMS deviation of the reflector, but also the focal length of the best fitting paraboloid, changes between the horizontal and zenith positions, as can be seen from Table 1. The position of the vertex of the best fitting paraboloid moves along the z-axis from +6.7 mm above the mechanical vertex ($z = 0°$) to −5.2 mm ($z = 90°$). These changes of focal length and position of the focal point, together with the changes in the RMS deviation of the reflector as a function of the elevation angle of the antenna, should result in a considerable increase in gain if the antenna is tilted from zenith to the horizon, an effect which tends in the same direction as the extinction of the atmosphere. No attempt has yet been made to measure the apparent extinction with the 85-foot telescope at a high frequency, and to separate the two effects.

Some conclusions can be drawn from these results which may be applied to future large antennas. Consider a RMS deviation of a parabolic reflector $\overline{D^2}(r)$ which depends on the distance r (normalized so that $r = 1$ corresponds to the edge of the aperture) from the antenna axis, and a tapered primary feed pattern which can be represented by $(1 - r^2)^p$. Then equation (13) for the weighted RMS deviation can be rewritten in the form

$$
(17) \qquad \overline{D^2} = \frac{2\pi \int_0^1 (1 - r^2)^p \, \overline{D^2}(r) \, r \, dr}{2\pi \int_0^1 (1 - r^2)^p \, r \, dr}
$$

The weight function $(1 - r^2)^p r$ reaches its maximum for

(18)
$$r_{max} = \frac{1}{\sqrt{2p + 1}}$$

which gives the value $(1 - \frac{1}{2p + 1})^p \cdot \frac{1}{\sqrt{2p + 1}}$ for the weight function.

This means, for example, that in the case p = 1 the RMS deviation at a distance r = 0.58 contributes most of the gain reduction, whereas the RMS deviations at r = 0.9 and r = 0.1 contribute only with 45% and 26%, respectively, of the maximum value. Hence, larger RMS deviations may be allowed in these regions.

As another application of the tolerance theory, let us consider a multifeed system at the NRAO 300-foot antenna with feeds spaced along NS direction. Because of physical limitations the closest possible spacing of the horn feeds at 1400 Mhz is 25 cm. With a focal length f = 39 m (Table 1), and a beam factor B = 0.873 (Table 2), this feed spacing means an angular separation of the corresponding main beams of

(20)
$$\Theta_{sp} = B \cdot arc\ tg \frac{\Delta f_{ax}}{f} = 0.873 \cdot 22.07 = 19.25'$$

which is approximately two times the HPBW of the antenna ($\Theta_A = 10'$). As may be seen from Figure 9 the theoretical gain reduction will be 2.5% for the first feeds (spaced $\pm 2\Theta_A$) and 11% for the second feeds (spaced $\pm 4\Theta_A$) as referred to the gain of the center feed. As also may be seen from the experimental values, the actual gain reduction may be considerably greater.

An inspection of Table 3 shows that the decrease of efficiency with decreasing wavelength is accompanied by an increasing main beam stray factor. This means that the main beam gain $G_m = \eta_R \frac{4\pi}{\Omega_m}$ in equation (16) is hardly affected by the RMS deviation of the reflector, but that the main beam stray factor β_m which measures the energy radiated (or received) outside the main beam increases with decreasing wavelength. This behavior has been predicted by tolerance theory [1], [5]. Measurements at two frequencies with the 25-m telescope of the Bonn University [11] have shown that this

increase of the main beam stray factor is mainly caused by an increase of the sidelobe attenuation in the immediate neighborhood of the main beam. This result is also in good agreement with the theoretical results obtained by Ruze and by Bracewell.

Acknowledgment

The author is indebted to Dr. J. Findlay and Dr. H. Hvatum for stimulating discussions.

References

[1]   Bracewell, R. N., Tolerance Theory of Large Antennas. IRE Trans. on Antennas and Propagation, Vol. AP-9, No. 1 (1961), pp. 49-58.

[2]   Yang, R., Quasi-Fraunhofer Gain of Parabolic Antennas. Proc. IRE (1955), p. 486.

[3]   Silver, S., Microwave Antenna Theory and Design. Radiation Laboratories Series, MIT, Vol. 12, McGraw-Hill (1949).

[4]   Kelleher, K. S., and H. P. Coleman, Off-Axis Characteristics of the Paraboloidal Reflector. NRL Report 4088 (December 31, 1952).

[5]   Ruze, J., Physical Limitations on Antennas. Technical Report 248, Research Laboratory of Electronics, MIT (October 30, 1952).

[6]   Parratt, Probability and Experimental Errors in Science. John Wiley and Sons, Inc., New York (1961).

[7]   Burke, B., Private communication

[8]   Wade, C., Private communication.

[9]   Barrett, A. H., Observations of Radio Sources at 1.8 cm Wavelength. Ap. J. 134, 945 (1961).

[10]   Findlay, J., Antennas and Receivers for Radio Astronomy. To appear in: Advances in Radio Research.

[11]   Mezger, P., Die Messung kleiner Rauschtemperaturen und die Messung der Eigenschaften einer 25-m-Antenne bei 1.4 and 2.7 GHz mit radio-astronomischen Mitteln. Forschungsbericht des Landes Nordrhein-Westfalen Nr. 1235 (1963).
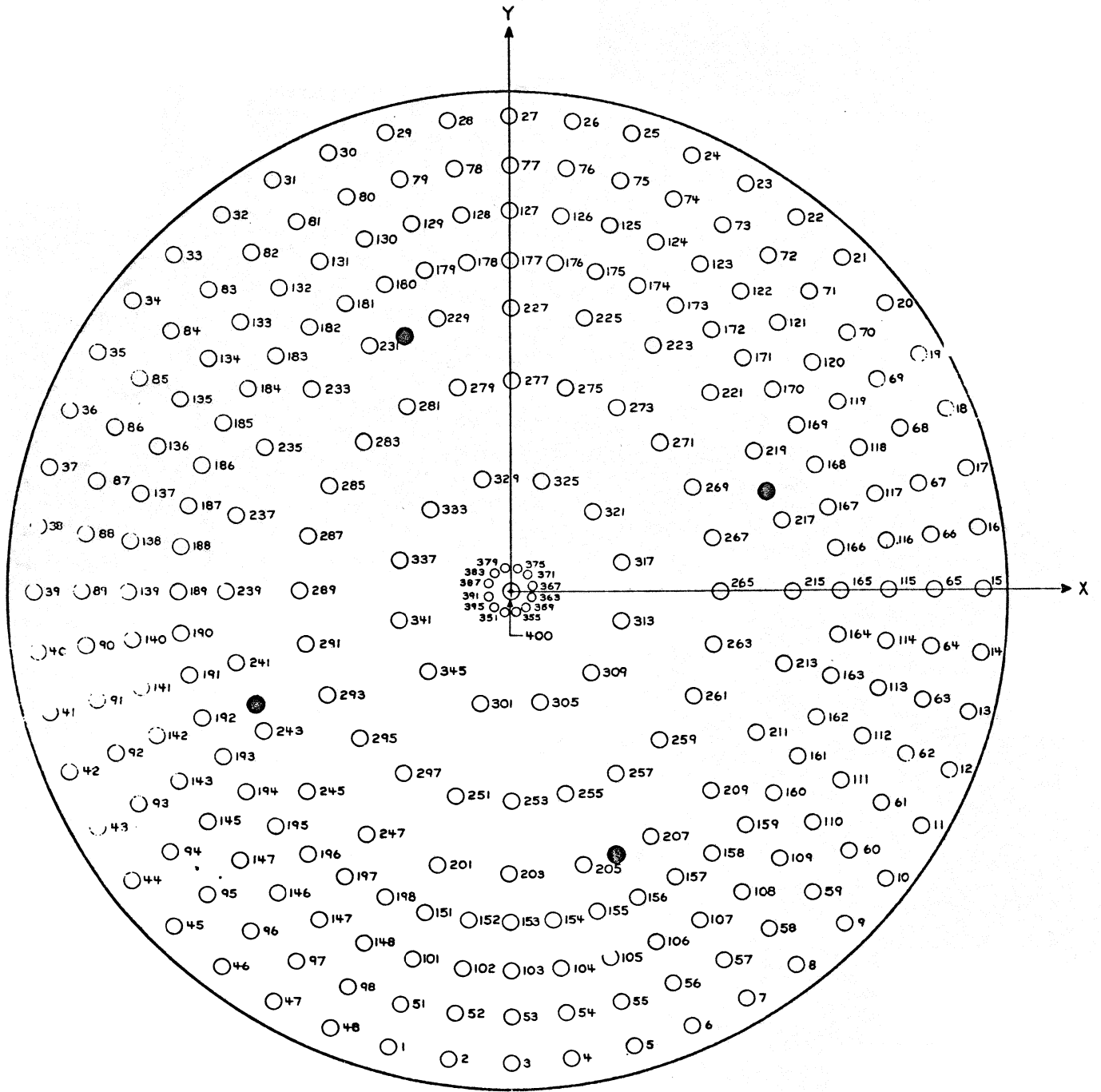
Figure 1. Position of the Target Points on the 85-foot Reflector
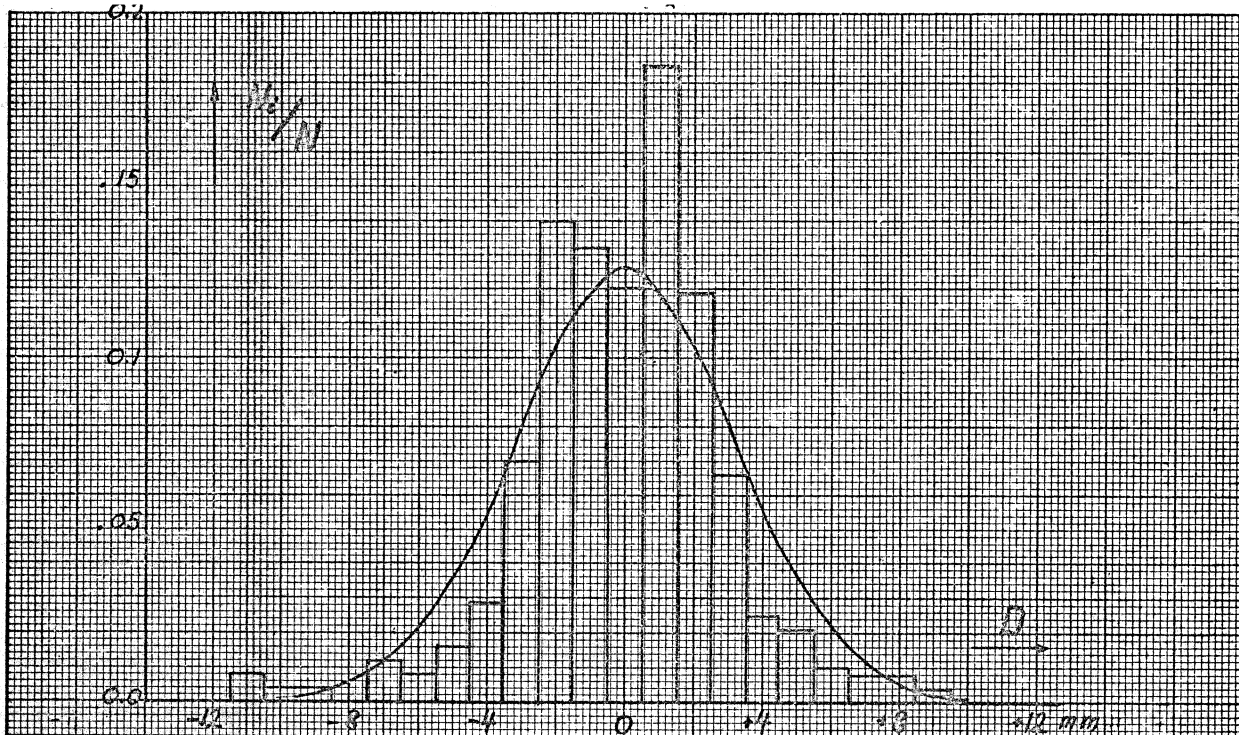
Fig. 2 a. The distribution of the measured deviations of the as-fit antenna from the best fitting paraboloid (N = 243 ; z = $\Theta°$)
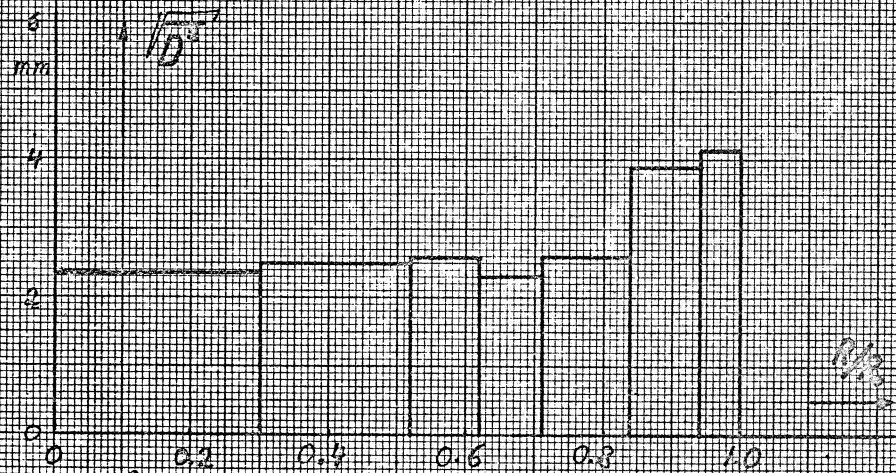
Fig. 2 b. The RMS value of the measured deviations from the best fitting paraboloid as a function of the distance R from the main axes of the paraboloid
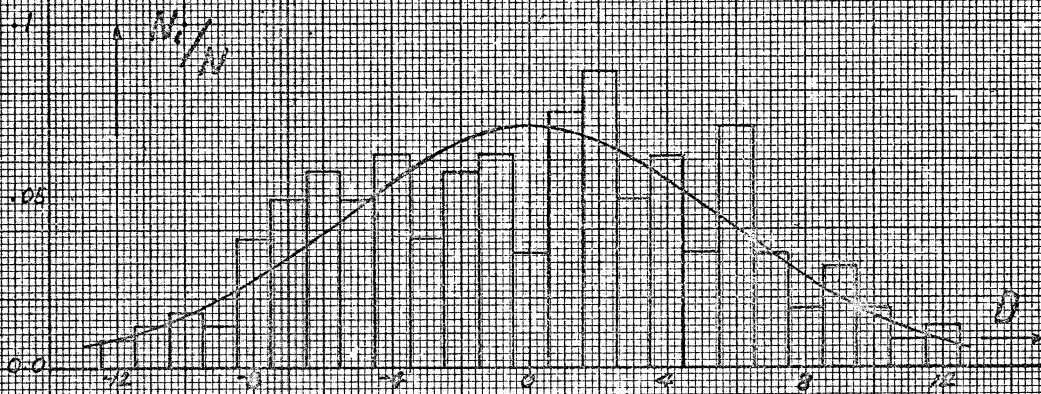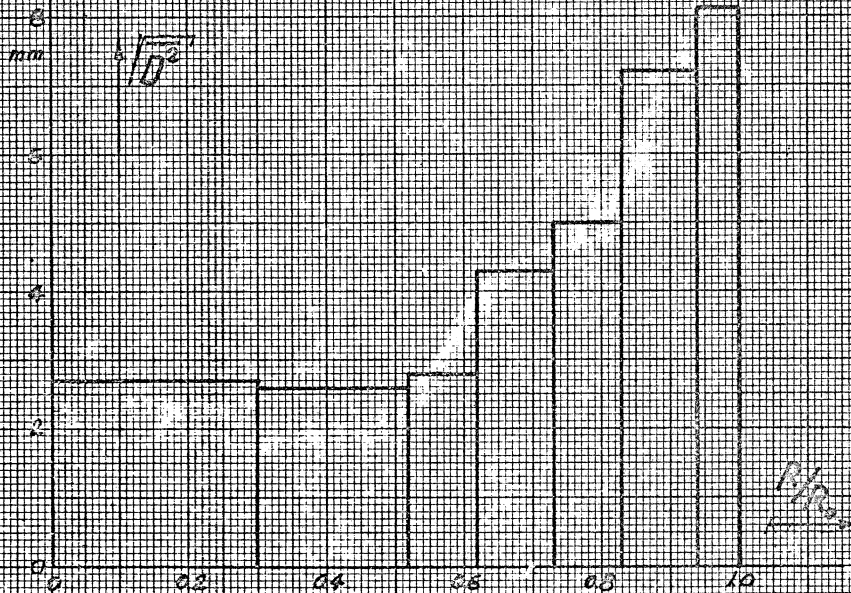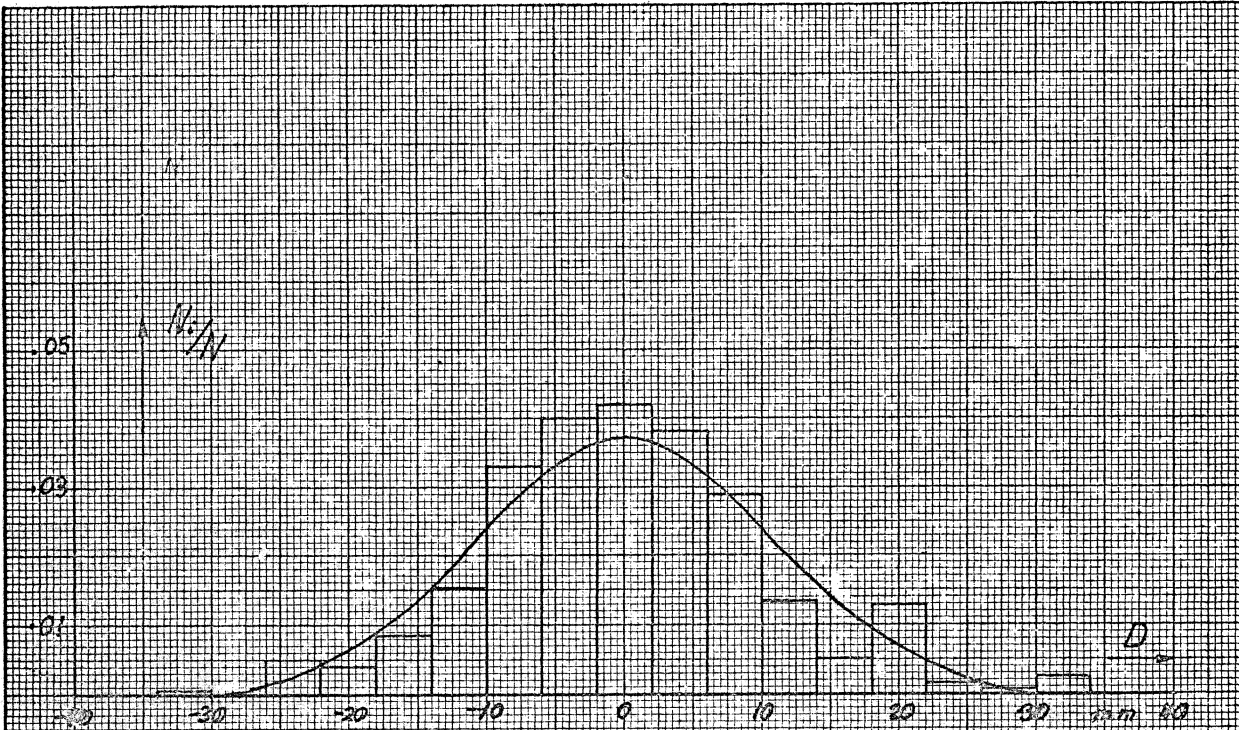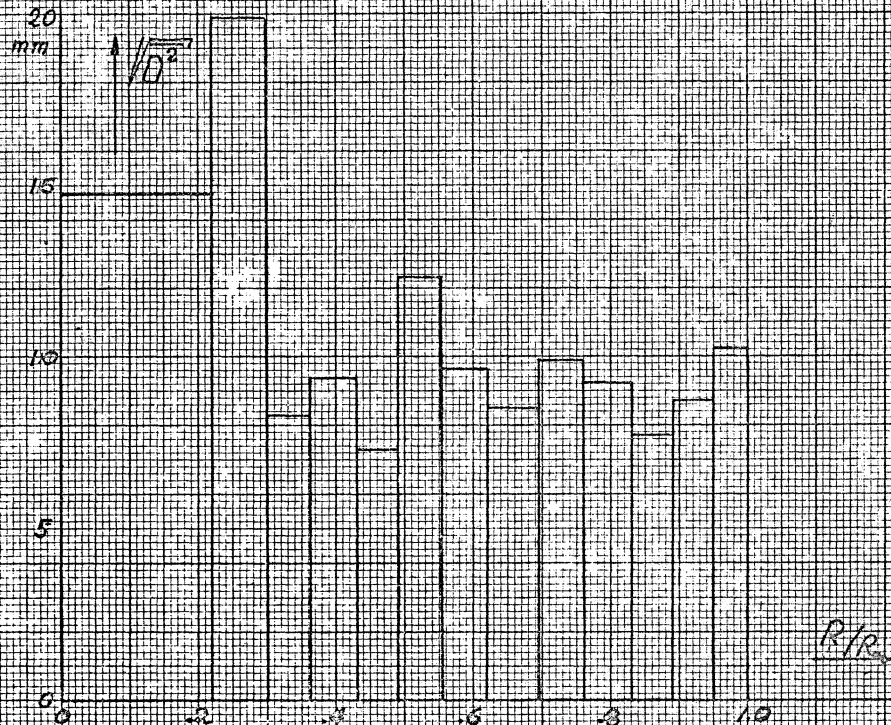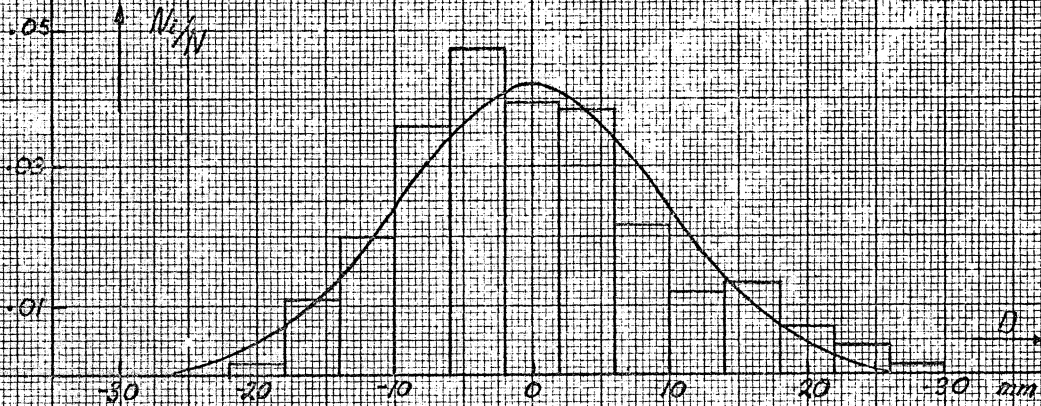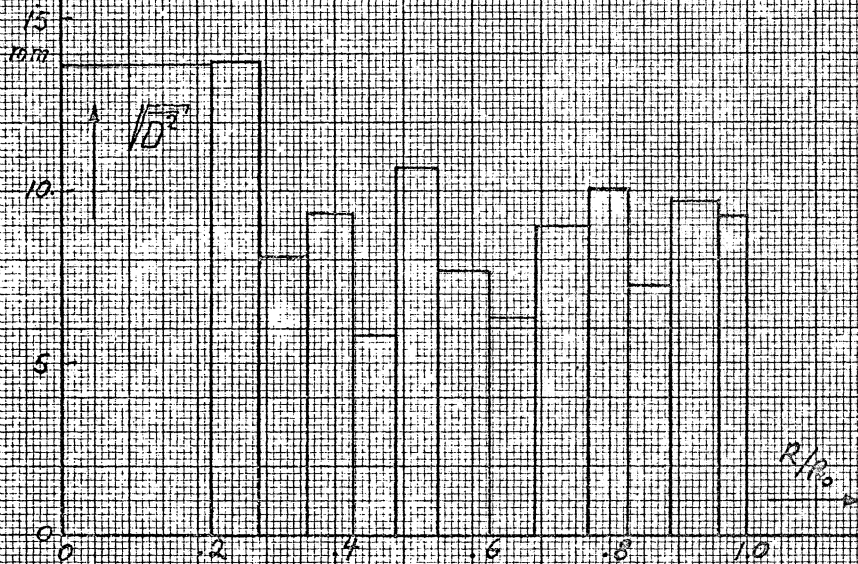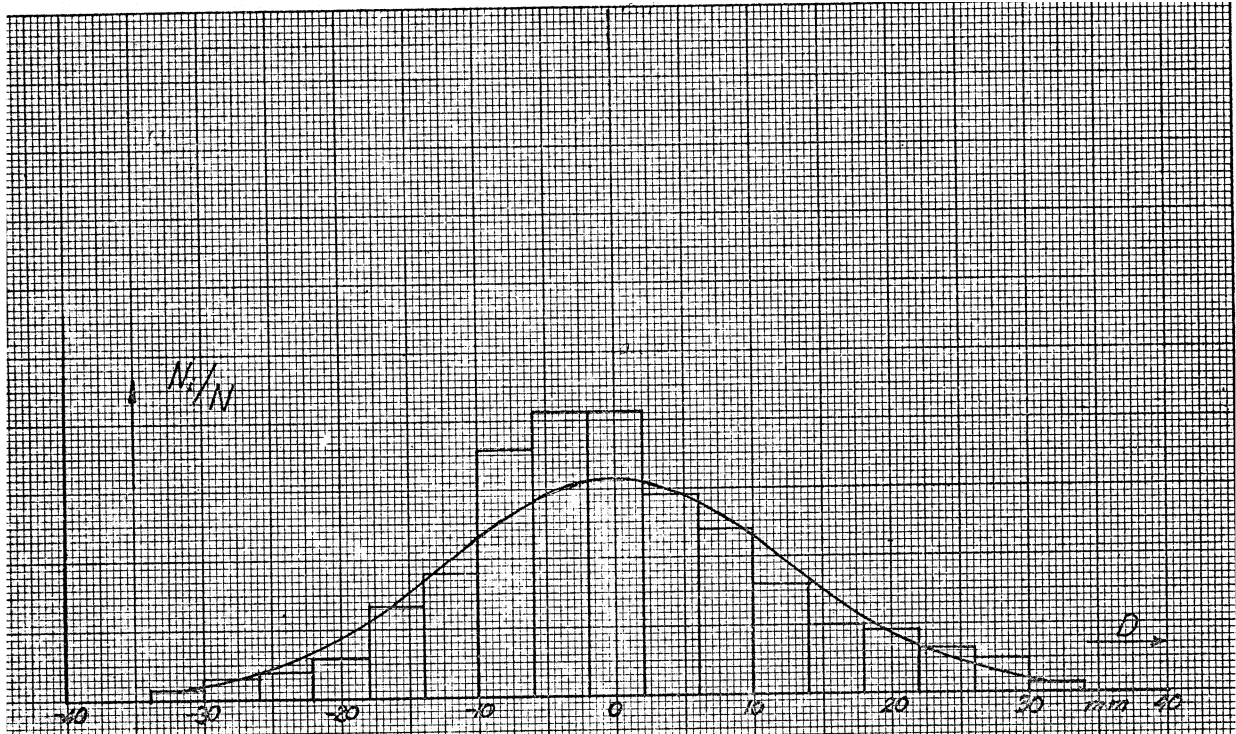
Fig. 3 a:The distribution of the measured deviations of the 25-ft antenna
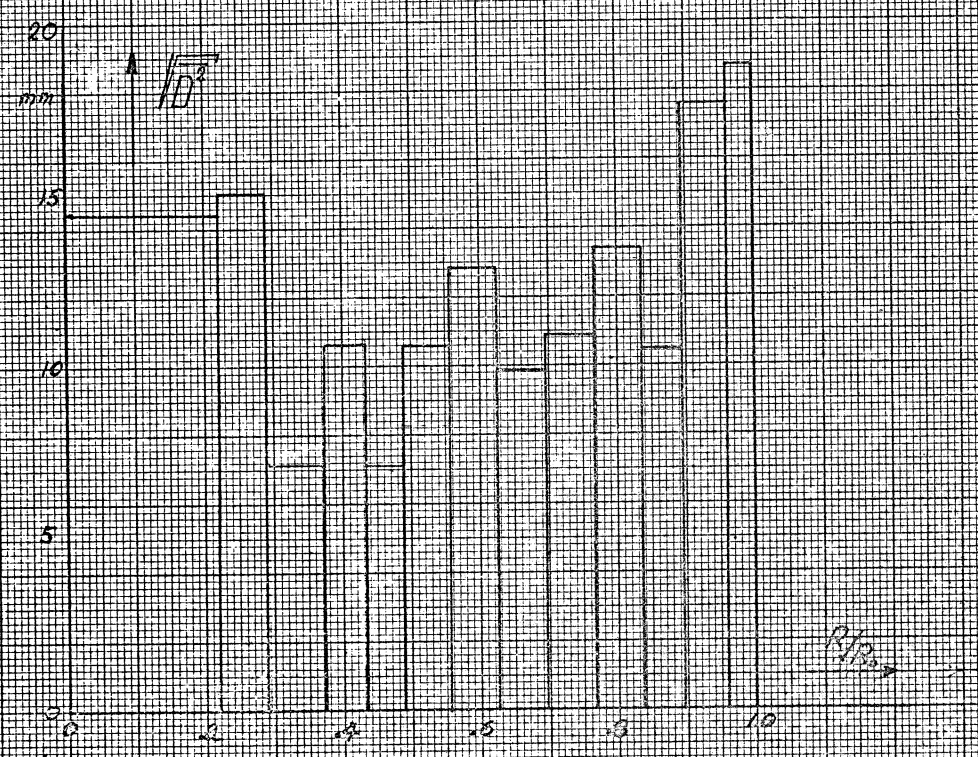from the best fitting paraboloid (N = 274   az = 90°)

Fig. 3 b:The RMS value of the measured deviations from the best
fitting paraboloid as a function of the distance R for
the main axes of the paraboloid

Fig. 4a: The distribution of the measured deviations of the 300-ft-antenna from the best fitting paraboloid (N = 293 ; u = 0°)

Fig. 4b: The RMS value of the measured deviations from the best fitting paraboloid as a function of the distance R to the main axis of the paraboloid

Fig. 5 a : The distribution of the measured deviations of the 300-ft-antenna from the best fitting paraboloid (N = 291, z = 30°)

Fig. 5 b: The RMS value of the measured deviations from the best fitting paraboloid as a function of the distance R from the main axes of the paraboloid

Fig. 6a : The distribution of the measured deviations of the 300-ft-antenna from the best fitting paraboloid (N = 293 ; z = 61°3040')

Fig. 6 b : The RMS value of the measured deviations from the best fitting paraboloid as a function of the distance R of the
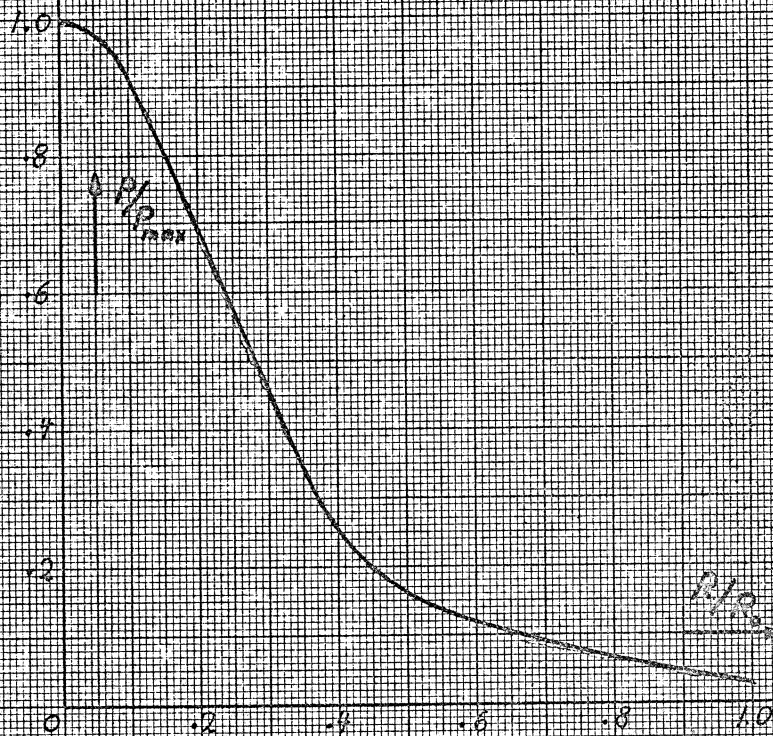
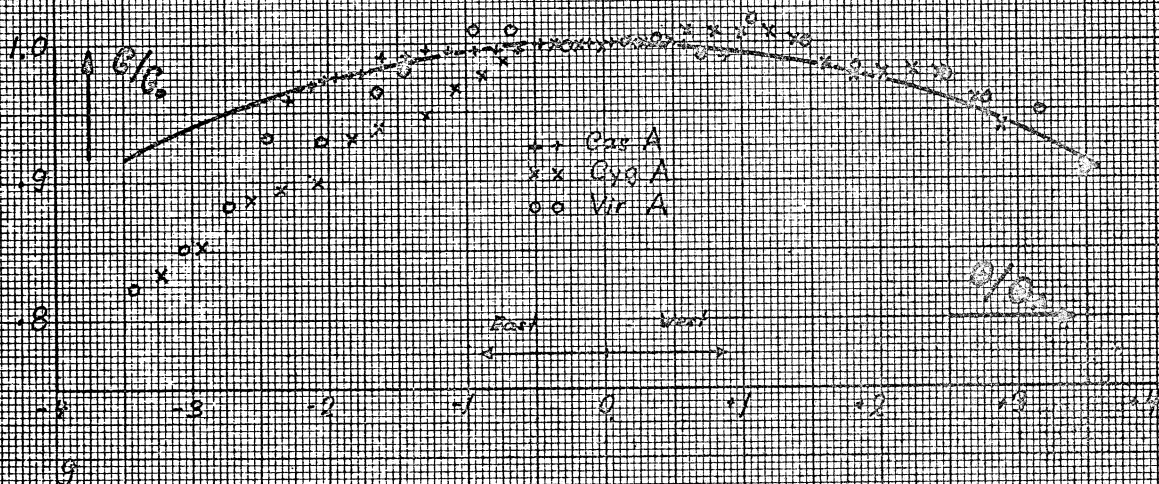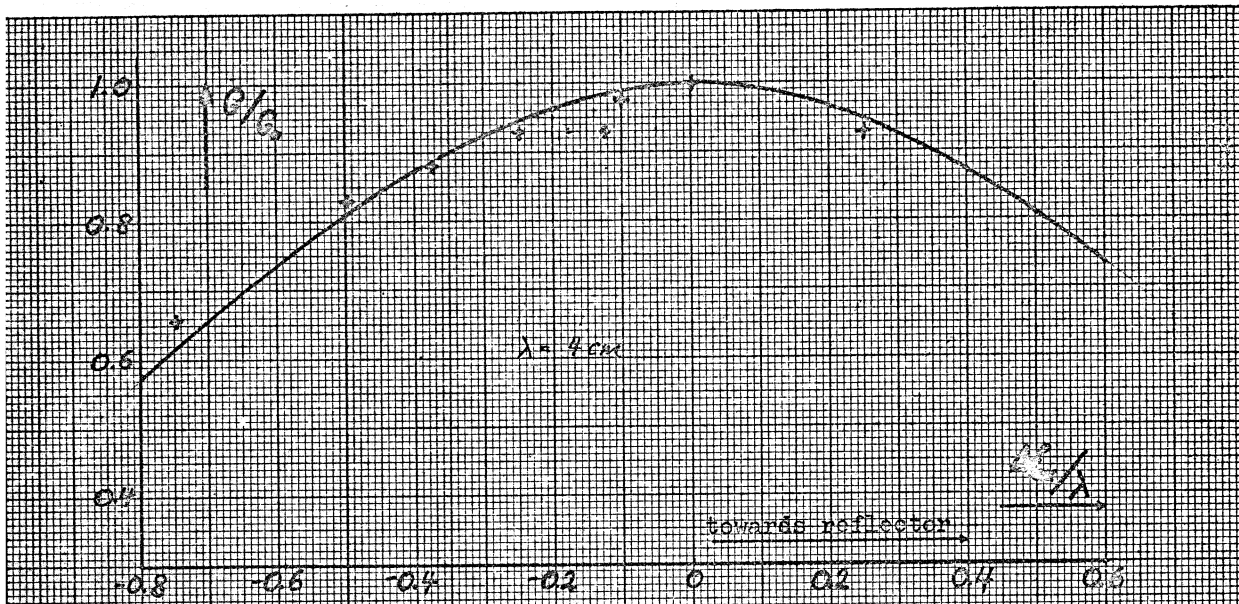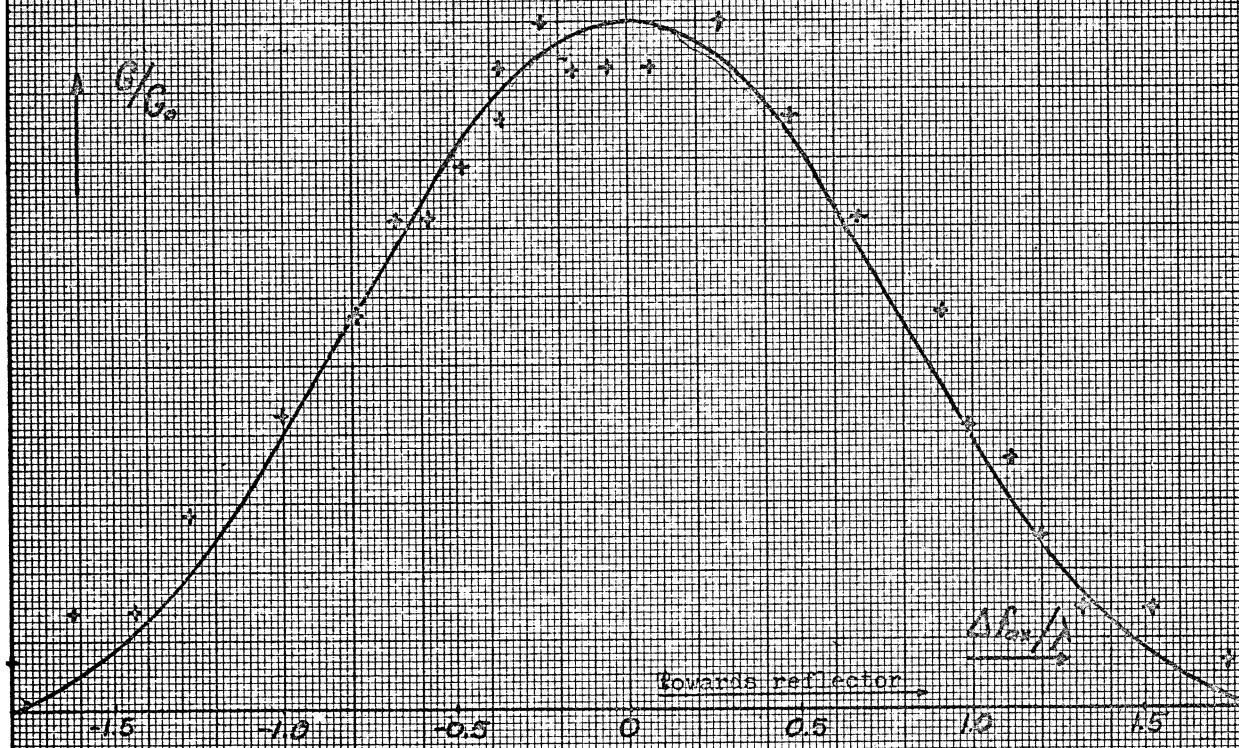Figure 7   Normalized primary pattern of the 25-foot reflector.

Figure 8.   Gain as a function of radial defocusing. Measured
points obtained with the 200-foot antenna.   The curve
interpolated from Silver's curves [3].
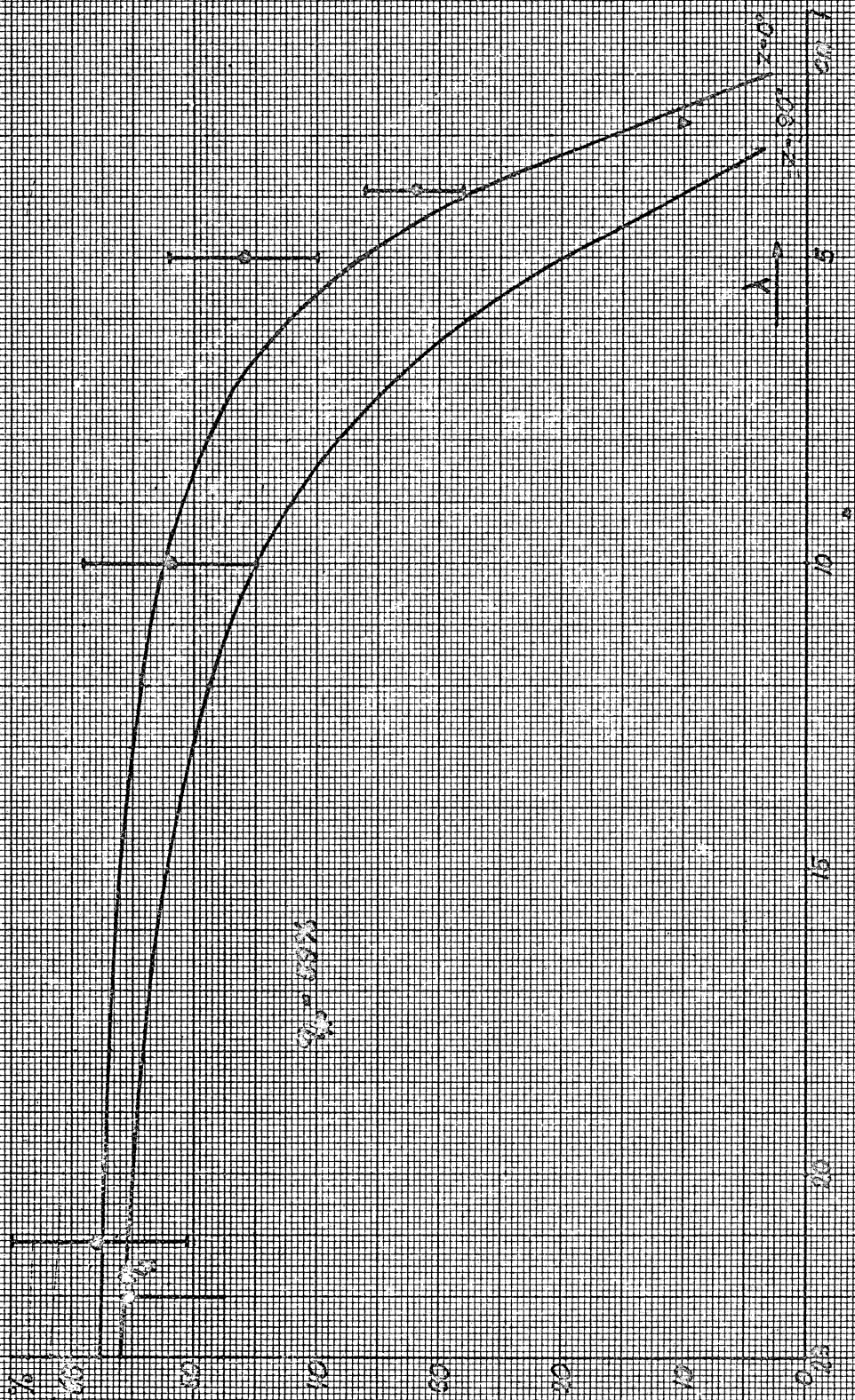
8a. Gain Variation as a Function of Axial Defocusing. +++ measured with
the 85-foot antenna at λ = 4 cm. Solid curve calculated from
equation (1a).

8b. Gain variation as a function of axial defocusing. +++ measured with the
85-foot antenna at λ = 6 cm. Solid curve calculated from equation (1a).

Figure 10. Contour map representation of the surface deviations of the 85-foot reflector from best fitting paraboloid measured in zenith position. Distances are measured in a direction normal to the reflector surface, positive direction towards the focal point. Interval = .005 ft., 1.5 mm.

Figure 11a. The aperture efficiency of the 85-foot antenna as a function of wavelength λ.

+ measured values estimated errors. Solid curves calculated from equation (30) with vertical RMS deviations from Table 1.
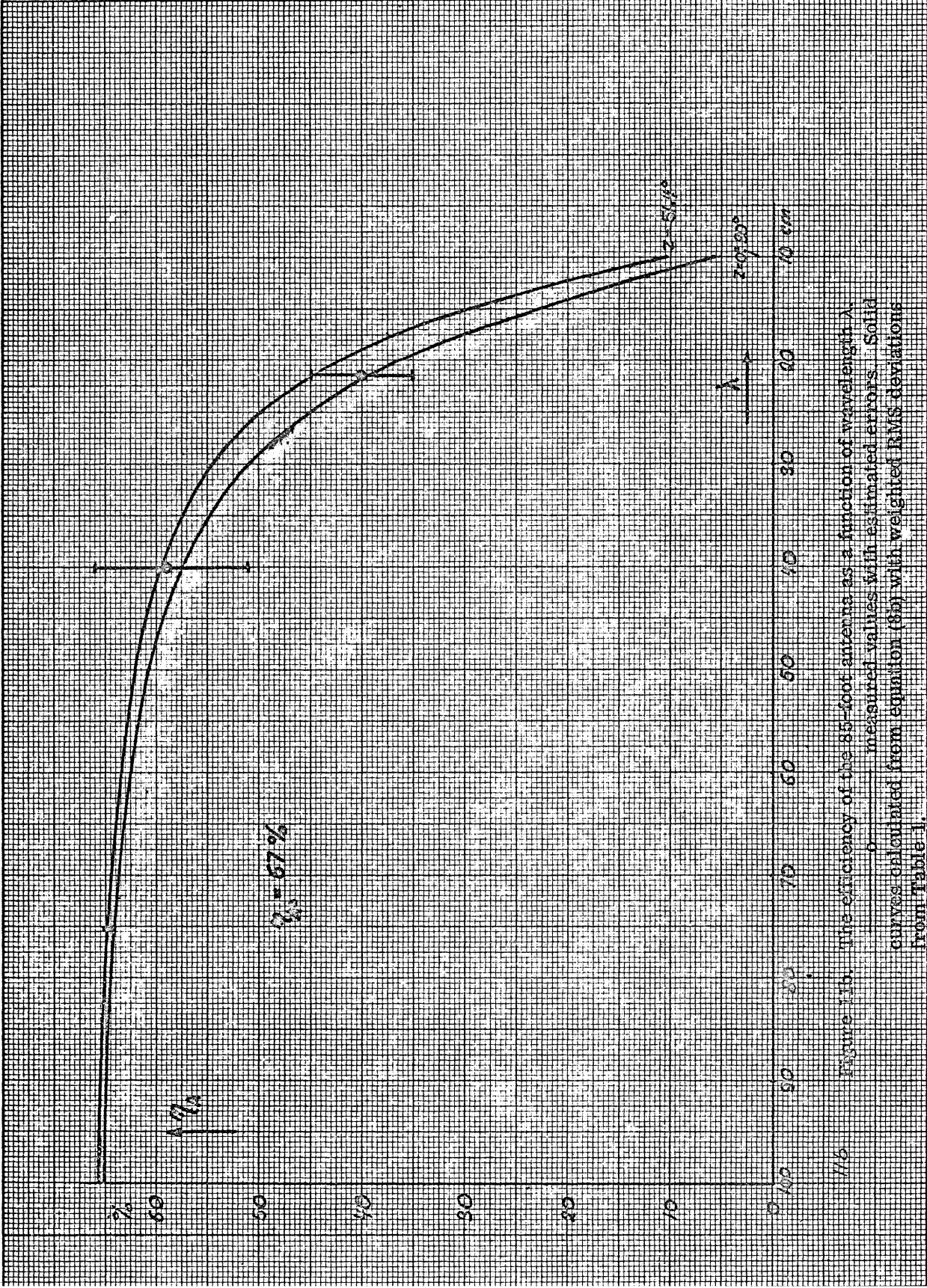○ measured values estimated errors.

Figure 11b. The efficiency of the 85-foot antenna as a function of wavelength λ.
Measured values with estimated errors. Solid
curves calculated from equation (11) with weighted RMS deviations
from Table 1.